ELECTROSTATIC DESIGN OF THE BARREL CRID AND ASSOCIATED MEASUREMENTS[*][‡]

K. Abe,[a] P. Antilogus,[b] D. Aston,[b] A. Bean,[c] T. Bienz,[b] F. Bird,[b**]
D. Caldwell,[c] P. Coyle,[d] D. Coyne,[d] J. Duboscq,[c] W. Dunwoodie,[b]
P. Gagnon,[d] D. Hale,[c] G. Hallewell,[b] K. Hasegawa,[a] J. Huber,[c]
P. Jacques,[e] R. A. Johnson,[f] H. Kawahara,[b] Y. Kwon,[b]
D. W. G. S. Leith,[b] A. Lu,[c] J. Martinez,[f] L. Mathys,[c] S. McHugh,[c]
R. Morrison,[c] D. Muller,[b] T. Nagamine,[b] M. Nussbaum,[f] T. Pavel,[b]
R. Plano,[e] B. Ratcliff,[b] P. Rensing,[b] A. K. S. Santha,[f] D. Schultz,[b]
S. Shapiro,[b] A. Shoup,[f] C. Simopoulos,[b] E. Solodov,[b♯] P. Stamer,[e]
I. Stockdale,[f] F. Suekane,[a] N. Toge,[b] J. Va'vra,[b] J. S. Whitaker,[g]
D. A. Williams,[d] S. H. Williams,[b] M. Witherell,[c] R. J. Wilson,[g]
S. Yellin,[c] and H. Yuta[a]

THE CRID GROUP

[a] *Department of Physics, Tohoku University, Aramaki, Sendai 980, Japan*
[b] *Stanford Linear Accelerator Center, Stanford University, Stanford, CA 94309, USA*
[c] *Department of Physics, University of California, Santa Barbara, CA 93106, USA*
[d] *Santa Cruz Institute for Particle Physics, University of California, Santa Cruz, CA 95064, USA*
[e] *Serin Physics Laboratory, Rutgers University, PO Box 849, Piscataway, NJ 08855, USA*
[f] *Department of Physics, University of Cincinnati, Cincinnati, OH 45221, USA*
[g] *Department of Physics, Boston University, Boston, MA 02215, USA*

ABSTRACT

We report on the electrostatic design and related measurements of the barrel Cherenkov Ring Imaging Detector for the Stanford Large Detector experiment at the Stanford Linear Accelerator Center Linear Collider. We include test results of photon feedback in TMAE-laden gas, distortion measurements in the drift boxes and corona measurements.

1. Introduction

A large Cherenkov Ring Imaging Detector (CRID)[1-3] is currently being installed in the Stanford Large Detector (SLD) experiment. We restrict our discussion to the barrel CRID (Fig. 1). It provides almost complete particle identification over 70% of the solid angle. By making use of both liquid and gaseous radiators $\pi/K/p$ separation will be possible up to about 30 GeV/c, and e/π separation up to about 6 GeV/c.
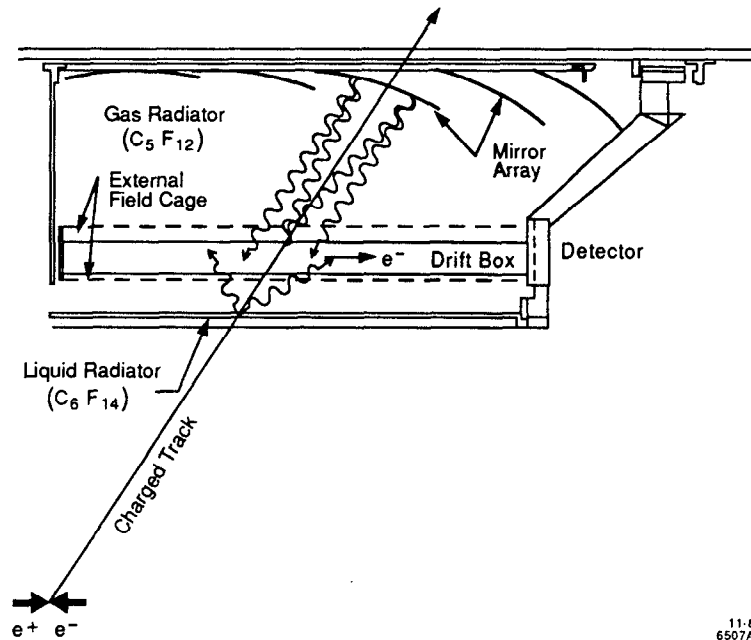

Figure 1: Basic concept of the SLD CRID barrel system.

Building of single electron detectors, drift boxes, mirrors and vessel have been finished, and they have been or are being installed. Building of liquid radiators, gas and liquid system, and electronics is in their final stages.

2. Single Electron Detector and the Photon Feedback

The construction and many tests of this device were described elsewhere.[4] Figure 2 describes its geometry, including a simulation of electron and positive ion gating. The arriving single electrons are detected by a plane of ninety-three 7 μm carbon wires, spaced at a pitch of 3.2 mm. Three production coordinates of the electron are measured from the drift time, the position of the wire giving the signal, and charge division along the wire. The measured resolution in each coordinate is about 1 mm, giving the CRID a high degree of reconstruction segmentation $d\theta/\theta = 4 \times 10^{-3}$.
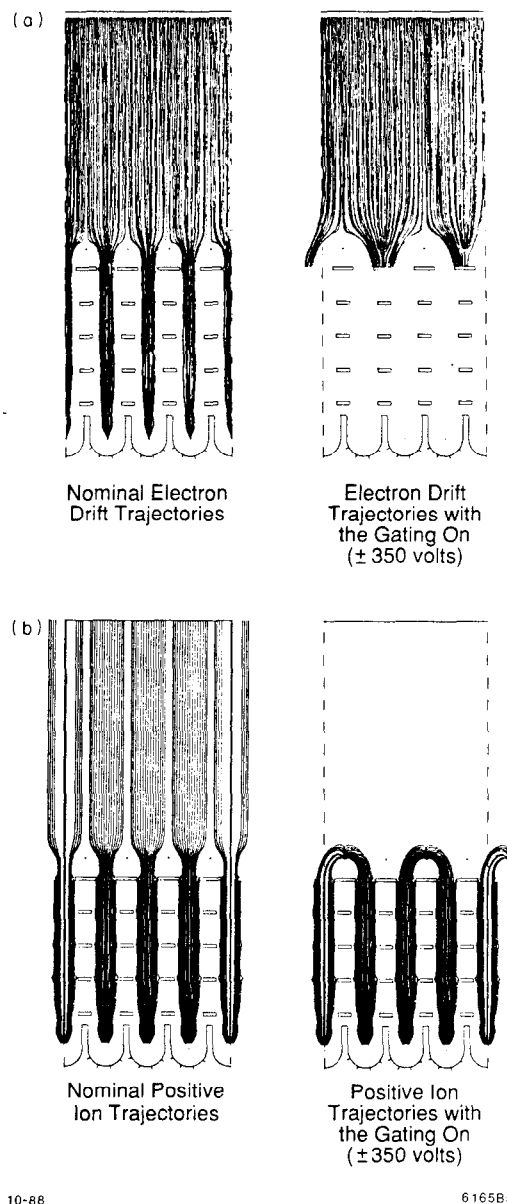
I

<div align="center">

(a)

Nominal Electron
Drift Trajectories

Electron Drift
Trajectories with
the Gating On
($\pm$ 350 volts)

(b)

Nominal Positive
Ion Trajectories

Positive Ion
Trajectories with
the Gating On
($\pm$350 volts)

10-88   6165B5

</div>

Figure 2: Geometry of the single electron detector, including its gating concept.

Ultraviolet photons are created by avalanche-excited carbon atoms.[5] Photons from excitations of hydrogen and nitrogen atoms are readily absorbed by the C_2H_6 carrier gas. However, Fig. 3 shows at least two C^* lines not absorbed in C_2H_6. Figure 3 shows that TMAE is especially sensitive to these photons and produces feedback electrons.

The single electron detector was designed primarily with the photon feedback in mind. The stack of five copper beryllium etched array electrodes (blinds), each 254 μm thick, limits the angle (6.6 degrees) over which photons from the avalanche
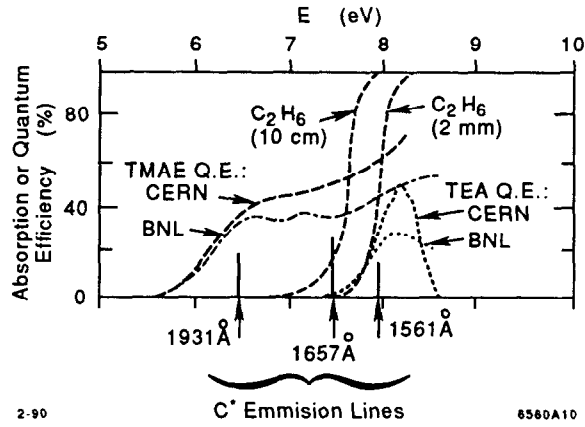
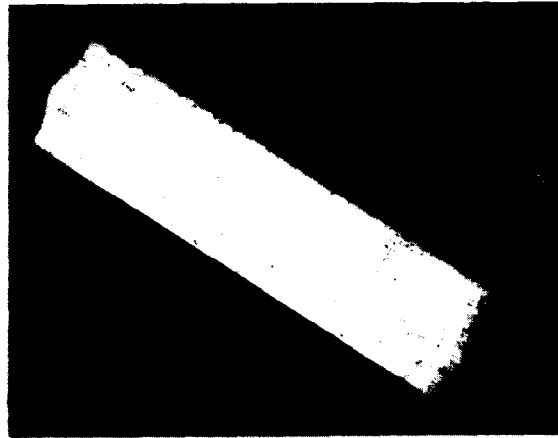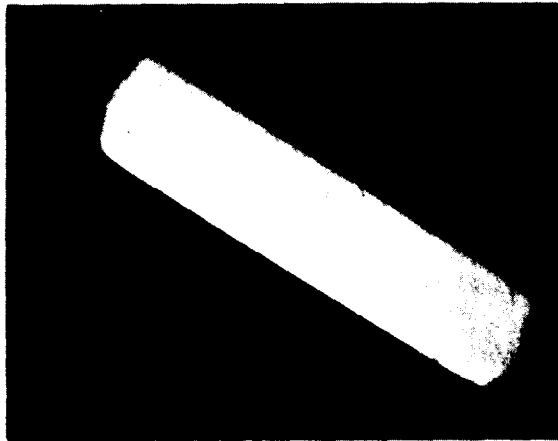<div align="center">3</div>

Figure 3: Sensitivity of TMAE to carbon excitation lines.

Figure 4: Cross section of etched Cu-Be blind electrodes used in the construction of the single electron detector, (a) before and (b) after electropolishing.
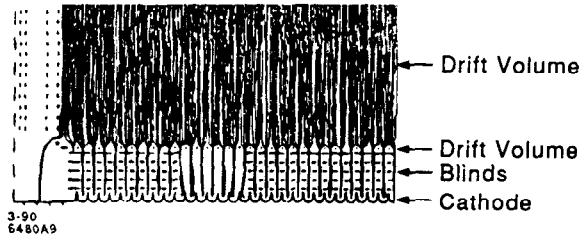
4

Figure 5: A special detector with modified etched array stack to study the photon feedback.

can reach the drift box volume. Each blind has 93 openings (2 mm wide), each centered above an anode wire. All five blinds are stacked on G-10 spacers and glued together to form a removable 15 mm thick package. Figure 4 shows a cross section of one such blind electrode before and after electropolishing. We have decided to electropolish these etched sheets because of fear of possible corona on the blind's sharp edges. Before the first blind, there is a wire plane (100 μm Cu-Be wires) which guides the drifting electrons into the openings in the etched sheets. In addition, this wire plane can serve as a gate to prevent positive ions from reaching the drift volume and photoelectrons reaching the anode. This is accomplished by pulsed biasing of the odd and even wires by $\pm$350 V.

To study the photon feedback, we constructed a special detector which had a modified etched array stack—see Fig. 5. In this detector the blinds were cut out in the middle of the stack, allowing us to compare the "blinded" and "nonblinded" regions. We left the gate wire plane undisturbed to preserve the correct coupling of the detector and the drift box electrostatic fields. Figure 6 shows our results. The primary electrons were generated by a low intensity laser beam entering perpendicularly into the drift box. Our acceptance window, to detect the secondary electrons, was between 100 ns and 4 μsec after primary arrival. One can see that the rate of the photon feedback correlates with the total charge produced in the avalanche, and this is independent of the TMAE content (temperature of the bubbler) or anode wire size. The difference between 12 and 28°C TMAE in Fig. 6(a) is caused entirely by a difference in gain between the two cases. We measure a rate of about 1 secondary electron per 100 avalanches in the "blinded" region at our nominal operating point, i.e., C_2H_6 gas with a TMAE bubbler temperature of 28°C and -1.45 kV cathode voltage. For the "nonblinded" region, this rate is about 6–8 times worse—see Fig. 6(b). The latter case would be unacceptable in the core of jets, because a typical charged particle leaves behind about 1000 electrons in the drift box volume due to its dE/dx interaction. The data points were corrected with the help of Monte Carlo program, to take into account the uninstrumented channels in the tails of the distributions.[6] The visible avalanche charge in Fig. 6(c) was integrated over 65 ns. The total average wire charge is about twice the average visible charge. At nominal operating point, the average total avalanche charge is 2×10^5 electrons.[4]
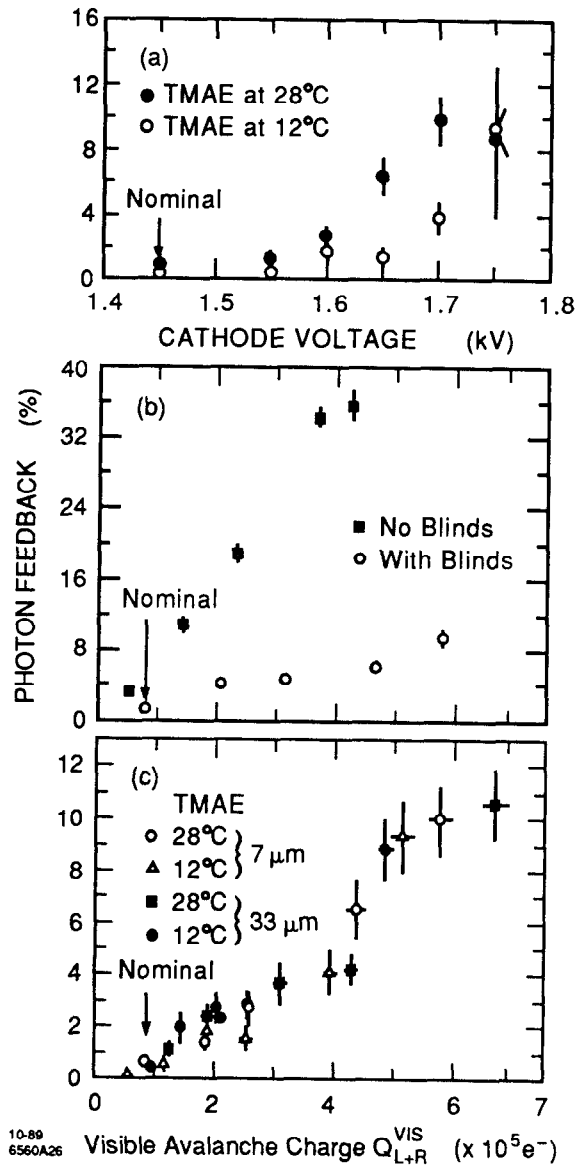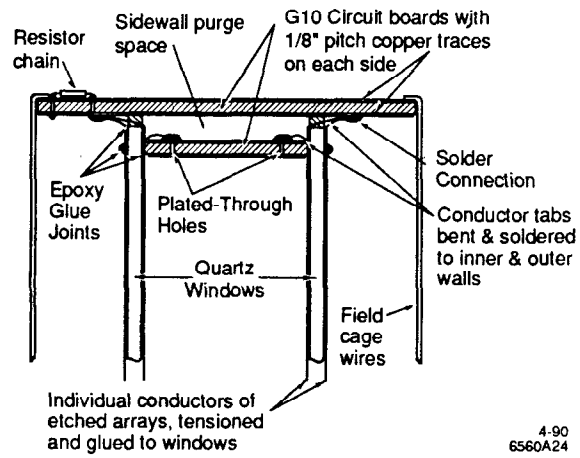
5

Figure 6: Results of the photon feedback study.

3. Drift Boxes and the Electrostatic Distortions

To ensure a uniform electric field in the drift box volume, graded-potential conductors are attached to both sides of the quartz window. Since the windows of the 40 drift boxes in the barrel CRID alone would require the stringing of about 63,000 wires, we have again used etched array technology. Large Cu-Be arrays (32 × 127 cm) were made up of conductors with cross-sections as described in Fig. 7; they were tensioned and glued on the quartz window. The conductors have 3.2 mm pitch. The interconnection of the etched array electrodes is illustrated in Fig. 8.
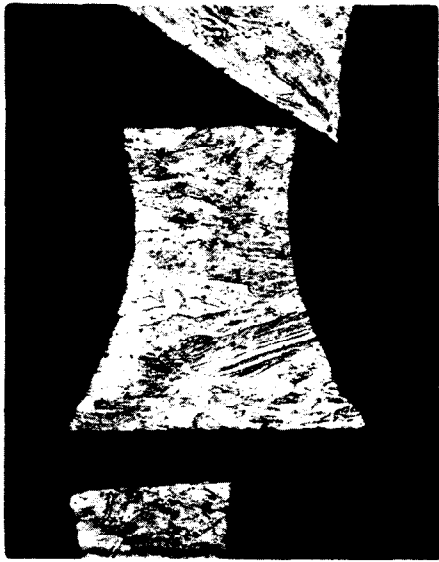
2-90   **6560A7**

Figure 7: Cross section of etched Cu-Be electrodes used in the construction of the drift boxes.

Resistor chain
Sidewall purge space
G10 Circuit boards with 1/8" pitch copper traces on each side
Epoxy Glue Joints
Plated-Through Holes
Quartz Windows
Solder Connection
Conductor tabs bent & soldered to inner & outer walls
Field cage wires
Individual conductors of etched arrays, tensioned and glued to windows

4-90
6560A24

Figure 8: Interconnection scheme of various electrodes in the drift boxes.

Epon 826 + Vers. 140
Scotchcast 226
Hexel 6103
DP 190 Drift Box #3
CIBA-GEIGY (508,6005,956) Drift Box #2

SURFACE RESISTIVITY (ohms / sq.)
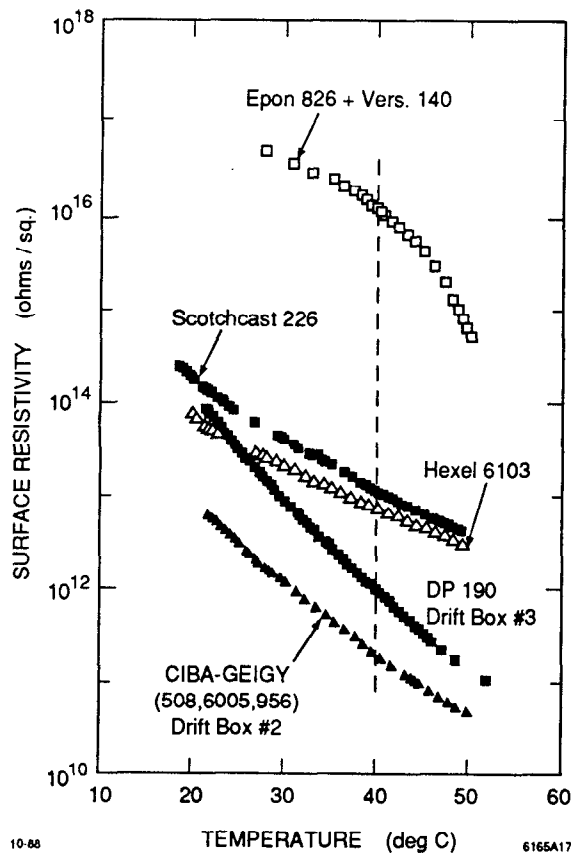TEMPERATURE (deg C)

10-88   6165A17

Figure 9: Measured surface resistivity of various glues as a function of temperature.[9]
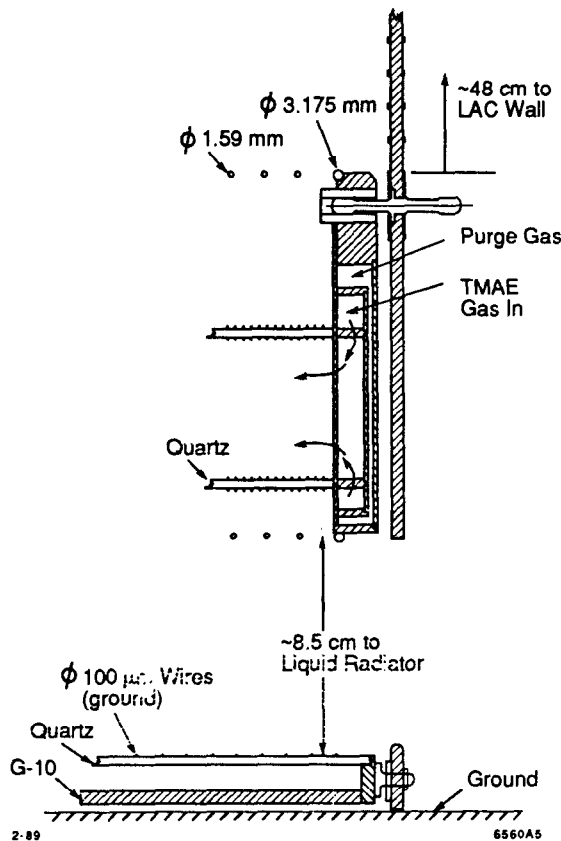
7

Figure 10: Electrostatic configuration of the drift box near the high voltage end.

The double layer G-10 design was driven by the need to prevent gas leaks between the etched conductors and the G-10 sides. The leak of C_5F_{12} at a level of few hundred ppb into the drift volume would have a catastrophic effect on the electron lifetime.[7] The G-10 sides had Cu strips on both sides and they were connected to the etched array electrodes. The potential grading was accomplished by two sets of four hundred 10 MΩ thick-film resistors (1% tolerance) soldered to the outer G-10 sheet. Spark gaps were added across every four resistors (100 gaps per drift box) in order to protect the 40,000 resistors in the barrel CRID system from being damaged by accidental sparks.

To ensure a good electron lifetime, one had to paint the inner G-10 sheet surface with some TMAE resistant glue.[8] The electrostatic properties could be severely affected if the glue had excessive surface and volume resistivity (for practical reasons one had to paint over the Cu strips). Figure 9 shows that at the expected operating temperature (40°C) the TMAE resistant DP-190 glue is within an acceptable range of surface resistivities, i.e., 10^{12} Ω (Ref. 2). (The volume resistivity drops similarly).[9] Figures 10 and 11 show the drift box design at high and low voltage ends. Clearly, the sharp edges of etched array conductors would cause severe corona problems at high voltage end of the drift box—see Fig. 11. Therefore we decided to add an additional field cage made of high quality Cu-Be rods. The nominal design assumes
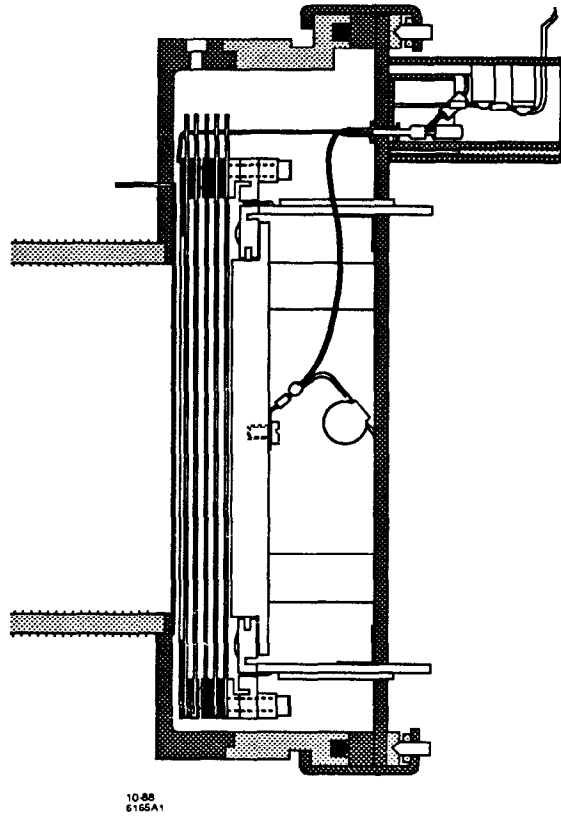
8

Figure 11: Electrostatic configuration of the drift box near the detector end.
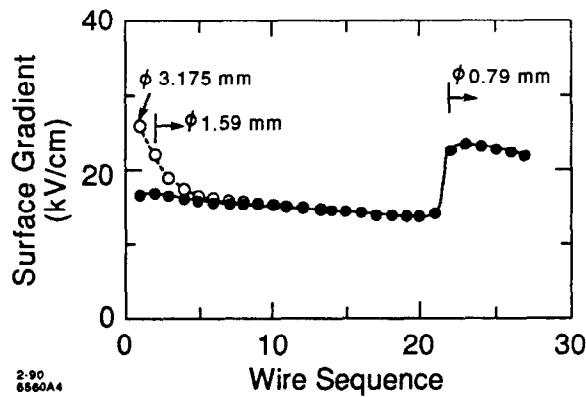

Figure 12: Distribution of surface gradients on the drift box field cage wires near the high voltage end (open circles correspond to one-sided loading of drift boxes with respect to the central plane).

that the liquid radiator wires will run at ground potential, although if necessary, they can be ran at a potential of 10 kV to reduce the stresses on the drift box field cage wires. Figure 12 shows a distribution of surface gradients on the field cage wires near the high voltage end, assuming 60 kV at highest end of the box. This is

9

an acceptable nominal design for an operation with the C_5F_{12} gas. We will discuss corona problems due to various defects later.

The finished drift boxes including single electron detectors were studied[10] in the setup described in Ref. 3. The setup includes a pulsed N_2 laser mounted on an x–y transport allowing it to be pointed into any region of the drift box. Here we will concentrate on the distortion measurements only. Figure 13 describes a principle to setup the voltages. First, we set the single electron detector voltages so that the electrons drift safely within its electrode structure, i.e., we are insensitive to a nominal misalignments and electrical gradients are safe from the operational point of view. Next the drift field in the drift box, say 400 V/cm, is set by adjusting the high and low voltage ends (the first Cu strip) of the drift box. However, at the same time we have to match the potential profile along the box sides with the one in the box middle, which is controlled by the detector's gate wire plane. Figure 13 shows a potential profile in the middle of the box along the lines going through the anode wire and the gate wire, after all voltages were iterated 3 or 4 times. Any electrode in the system must agree with this potential profile, otherwise a distortion occurs. We have set the voltages according to this recipe and found experimentally that no additional correction was necessary.

Figure 14 shows distortions measured across the width of a drift box, for several drift distance. The plot shows the measured position minus the predicted position, in millimeters. The distortions are largest near the G-10 side wall, for x near 0 and 300 mm, but even there they do not exceed 2 mm.

Figure 15 shows distortion along the z-direction in the middle of the box, i.e., along the box depth. The laser beam was inclined in this measurement. The z-coordinate was measured by charge division. Similar measurements 1.5 cm from the sides show distortions of up to 5 mm in the corners of the drift volume, with 2 mm being a more typical value.

Figure 16 shows what happens if we depart from the "matched voltage solution" (Fig. 13), i.e., if we mismatch the drift field in the drift box and the detector by ±200 V by adjusting the first Cu strip on the drift box. A very large distortion occurs which agrees with the corresponding calculation using our electrostatic program.[11]

4. High Voltage System and Corona Measurements

The CRID group decided early in the experiment not to pursue a volume degrader solution. Thus, the high voltage problem was transferred from the intricacies of the volume degrader to possible corona problems. As we said, the nominal design has no problem—see Fig. 12. However, the trick is to ensure that the system of about 7000 field cage wires in the barrel CRID have no defect. Similarly, one should worry about defects on the drift box outer G-10 sides facing the liquid radiators, or broken etched array wires hanging from the boxes. Last but not the least, the central plane supporting the drift boxes—see Fig. 17—has to be supported by 20 ceramic insulators and they, too, have to take the high voltage stress also. To test
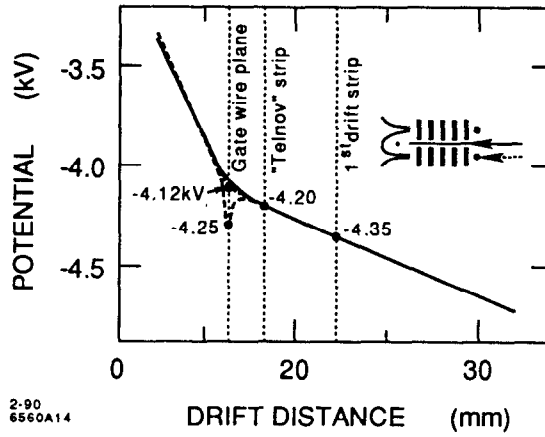
10

Figure 13: Principle of matching the drift box and the detector voltages.
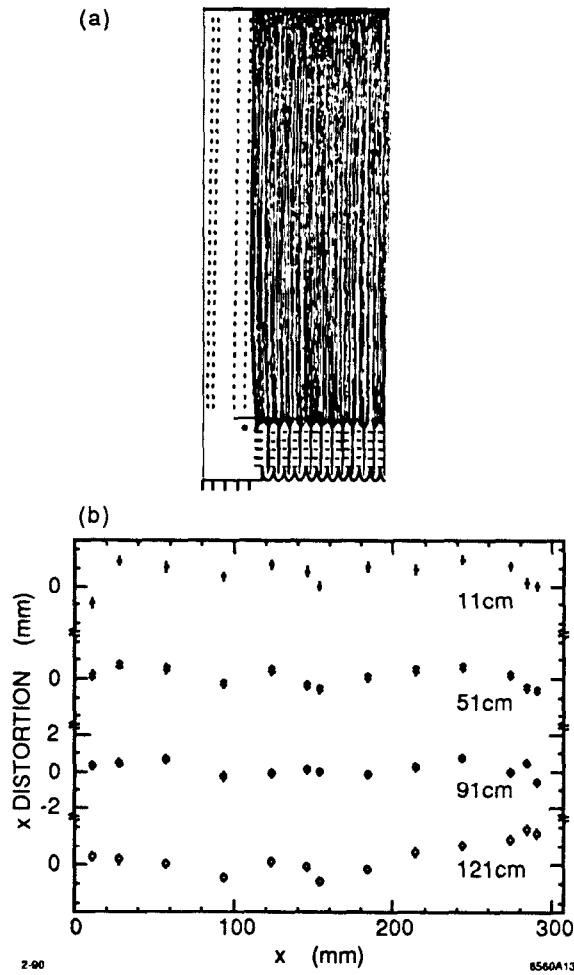

Figure 14: Difference between the expected and measured x position for different values of x across the width of CRID drift box, and for various drift distances.
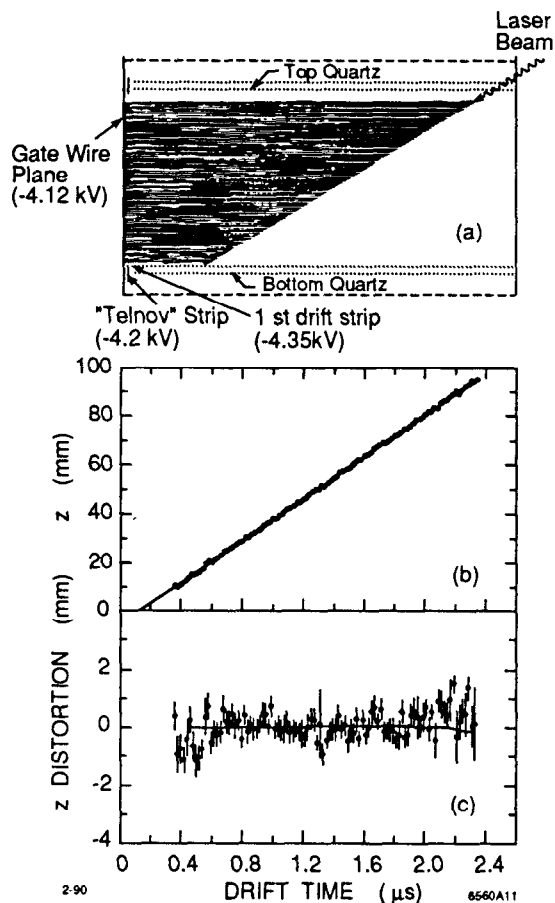
Figure 15: Use of an angled laser track to investigate z distortion along the drift box depth. The residual distribution (c) is for the nominal operating voltages.

some of these issues, we constructed a high voltage test setup simulating closely the barrel CRID geometry.[12] This allowed us to introduce defects at various spots of the structure. Figure 18 shows the corona effect due to a simulated broken etched array wire hanging from the box and facing the liquid radiator side. One can see that the corona in air is already noticeable at 10–15 kV as an extra current, and as an increased noise rate from the loop antenna facing the box. We have shown that prolonged corona can reduce the transmitivity of the quartz.[13] All 40 drift boxes are tested in this setup. This test setup also showed that it was necessary to bake the Mycalex ceramic insulators at 300°C to ensure adequate surface resistance uniformity and thus proper high voltage behavior. We also learned how to bring the high voltage into the central plane bus—see Fig. 19. A failure of this particular cable would be a major disruption of the CRID operation, as it would be necessary to dismantle some mirrors and some drift boxes in order to gain access. Figure 20 shows a controlled measurement of corona in a geometry where a needle of 30 μm radius at the tip faces a flat electrode 5 mm away.[12,13] One can see a relative comparison of onset of corona for air and C_5F_{12}, and for negative and positive voltage
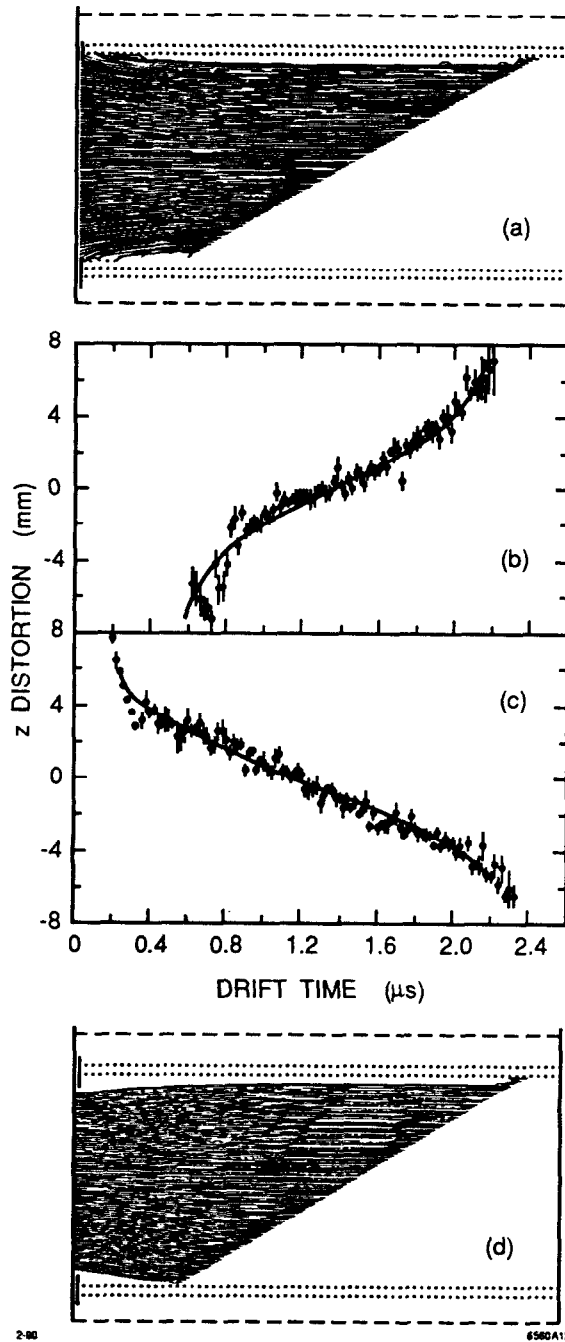
12

Figure 16: Effect of a mismatch in voltages between the drift box (first drift strip) and the detector (gate wire plane) by ±200 V. The curves are the predictions of the electrostatic simulation.

on the needle facing grounded flat electrode. The former configuration simulates the possible corona on the drift box field cage wires, the latter simulates a corona on the liquid radiator wires. The important point is that although the C_5F_{12} gas certainly helps, it will not save us if a defect's field gradient exceeds a certain value. There-
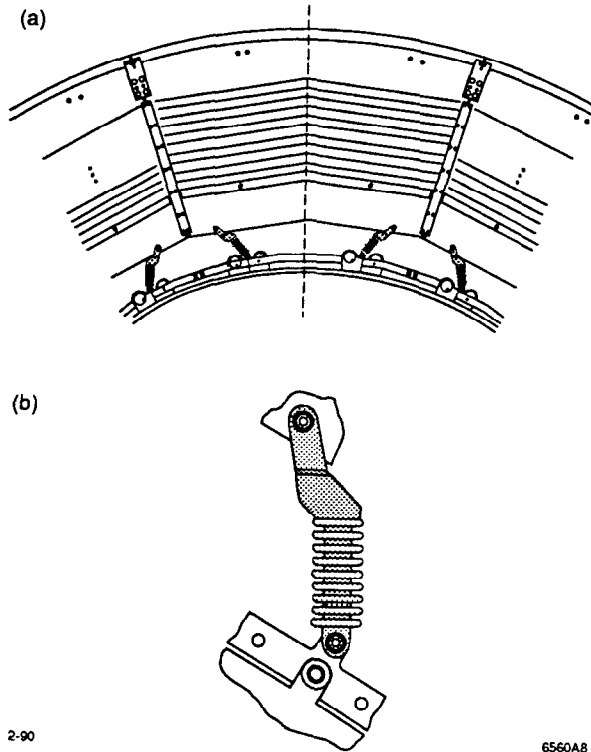
13

Figure 17: A concept of (a) central high voltage plane and (b) ceramic standoffs supporting it.
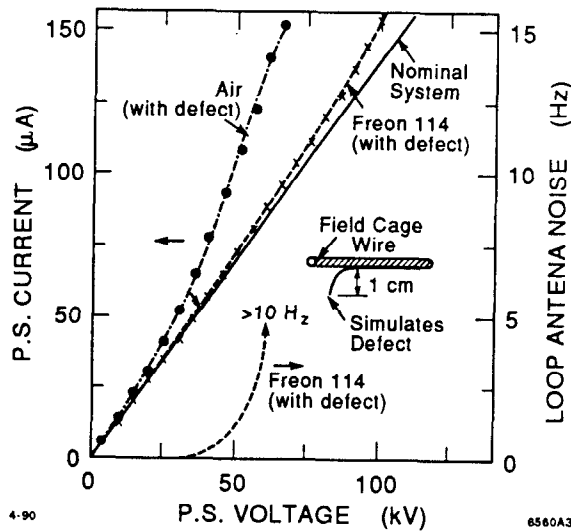

Figure 18: An onset of corona caused by a broken etched array electrode pointing towards the liquid radiators.

fore it is absolutely a must to catch all defects before installation of the drift boxes into the vessel. All drift boxes are tested in air up to a voltage a 60 kV. Several boxes
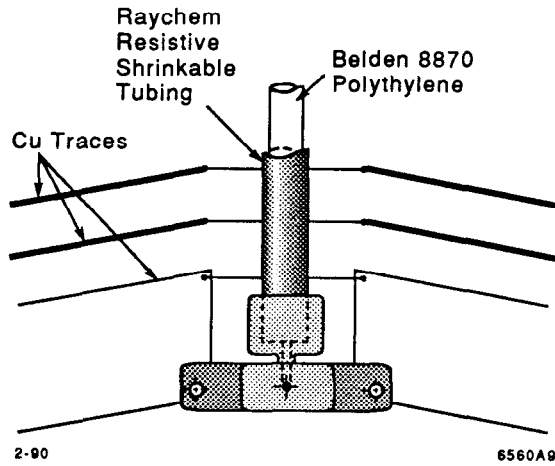
14

Figure 19:   A concept of bringing the high voltage to the high voltage bus of the central plane.
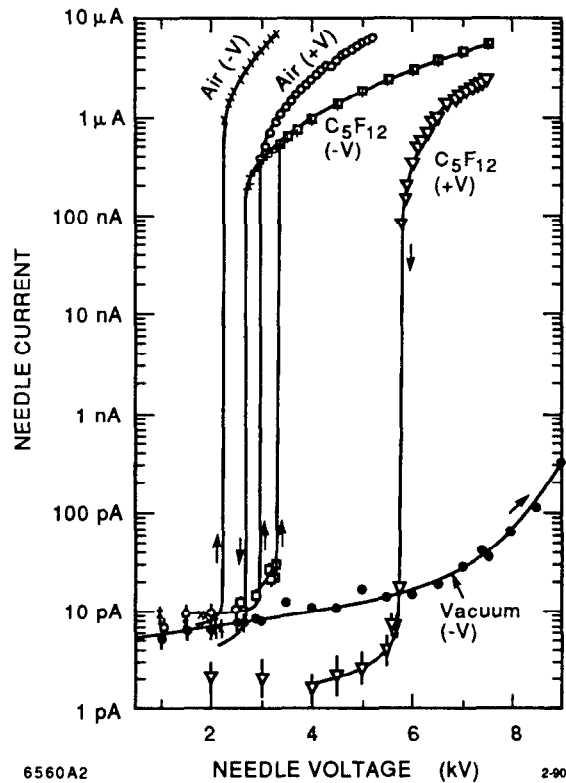

Figure 20:   Corona current for C_5F_{12} and air at 1 atm; needle has about 30 μm radius at the tip, which is 5 mm away from a flat electrode.

were tested for many months in Freon-114, which has similar high voltage behavior to C_5F_{12} gas.

Figure 21 shows the basic concept of the barrel CRID high voltage distribution system. Its safe operation at 60 kV depends critically on a system of 20 corona
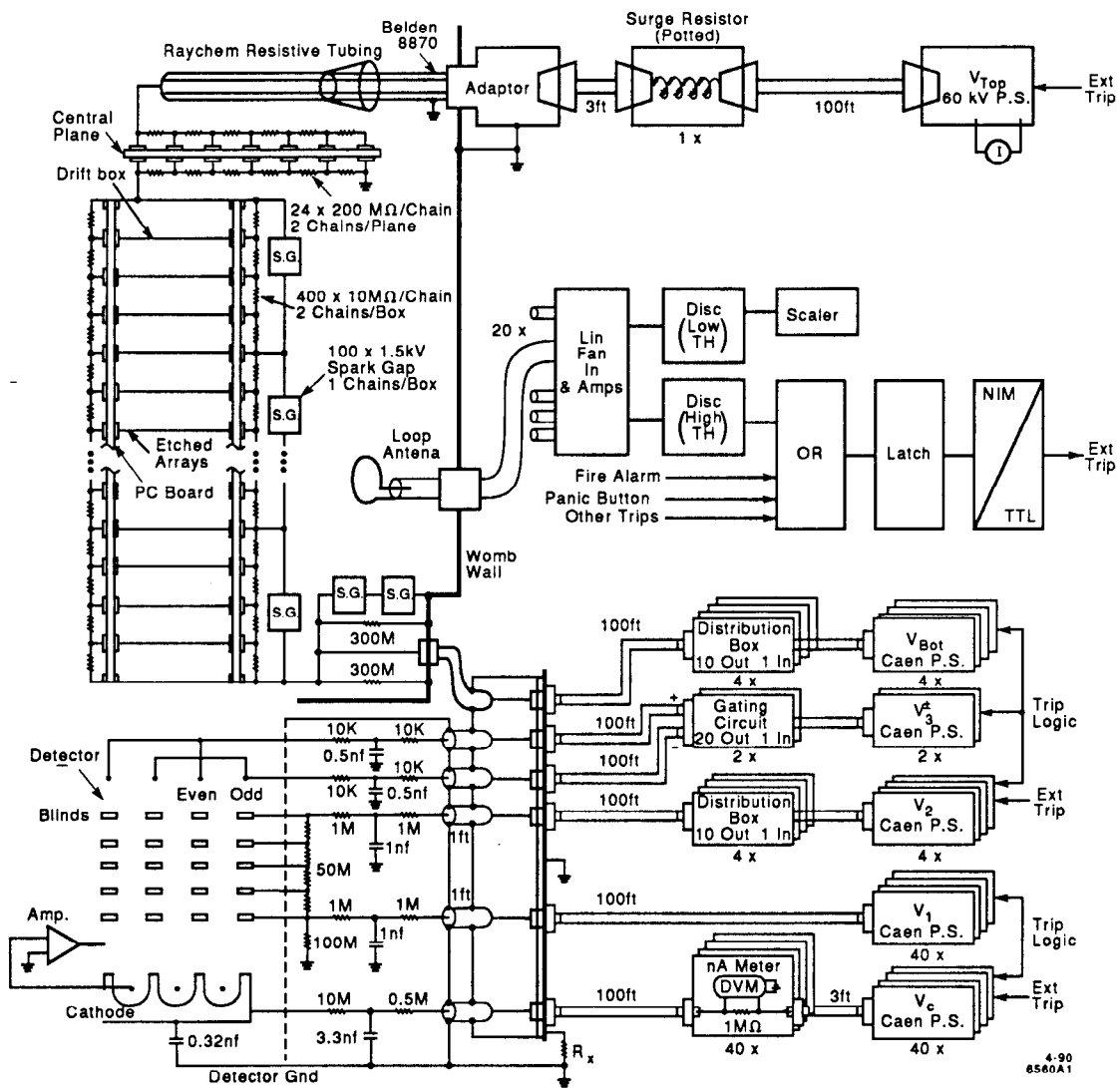
15

Figure 21: A basic concept of the barrel CRID high voltage distribution system.

antenna loops installed in the vessel, which are supposed to detect an onset of the corona and shut the whole system down if the pickup amplitude exceeds a certain threshold. A 60 kV current limiting resistor is made from 60 carbon resistors wound in a spiral form and vacuum potted. The single electron detector cathode currents can be monitored down to a nA level by a system of battery powered floating miniature DVM's.

References

1. SLD Design Report SLAC–REPORT–273, UC–23D (1984), and later revisions.

2. D. Aston et al., *Nucl. Instrum. Methods* **A283** (1989) 582.

3. M. Cavalli-Sforza et al., *IEEE Trans. Nucl. Sci.* (1990).

4. D. Aston et al., *Nucl. Instrum. Methods* **A283** (1989) 590;
   J. Va'vra et al., *IEEE Trans. Nucl. Sci.* **NS–35** (1988) 487.

5. H. Morgan and J. E. Mentall, *J. Chem. Phys.* **60,** No. 12 (1974).

6. D. Muller et al., CRID Note #58 (1990).

7. D. Fraissard et al., *Nucl. Instrum. Methods* **A252** (1986) 524.

8. M. Cavalli-Sforza, CRID Note #15 (1986).

9. J. Va'vra, Appendix to CRID Note #36 (1988).

10. P. Coyle et al., CRID Note #62 (1990).

11. S. Dasu, CRID nNote #63 (1990).

12. J. Va'vra, CRID Note #66 (1990).

13. J. Va'vra, "Aging of Gaseous Detectors," *Proc. Vth Int. Conf. on Instrum. for Colliding Beam Physics,* Novosibirsk, USSR, 1990; SLAC–PUB–5207 (1990); CRID Note #38 (1987).